Part II

Harmonic and super-harmonic sloshing dynamics of orbital-shaken cylindrical reservoirs

Introduction

Sloshing, i.e., the oscillations of a free liquid surface in partially filled containers, is an important issue in mechanical and aerospace engineering as well as in daily life. For instance, casually shaking a glass of water or a cup of coffee may lead to unpleasant liquid spilling (Mayer and Krechetnikov, 2012) (see figure II.1(a)). Closer to engineering, the total weight of launch vehicles and road or ship tankers is constituted in a large percentage by the liquids transported and by fuel. As the sloshing frequencies might be close to the control system frequencies, possible resonant sloshing dynamics can induce significant displacements of the vehicle's center of mass, thus endangering its dynamical stability (Ibrahim, 2005), with critical consequences on the transport safety and vehicle's performances (see figure II.1(b).

In some other applications however, enhancement of sloshing waves is seen as beneficial (see figure II.1(c)): in biology for example, cellular growth takes place in nutritive media placed into bioreactors (McDaniel and Bailey, 1969; Wurm, 2004). These containers are agitated so as to mix the liquid, prevent sedimentation and enhance gas transfer, which provides suitable oxygenation to the growing cell population (Klöckner and Büchs, 2012).

Therefore, a proper predictive understanding and modelling of the sloshing hydrodynamics at stake is essential in the design process of liquid tanks, so as to implement active control systems of vehicles and ensure efficient mixing processes.

For moderately large-size containers, sloshing is classically modelled by determining the oscillation modes compatible with a given tank shape using potential flow theory supplemented by viscous dissipation coming from bulk potential flow and Stokes boundary layers along walls (Faltinsen and Timokha, 2009). More precisely, gravity waves are restricted into modes with a discrete set of wavenumbers, owing to the action of the container walls. The values of the associated natural frequencies depend on the geometrical and fluid parameters through the well-known dispersion relation for capillary-gravity waves (Lamb 1932),

$$\omega_{mn}^2 = g k_{mn} \left(1 + \gamma k_{mn}^2 / \rho g\right) \tanh\left(k_{mn} h\right), \tag{3.72}$$

where g is the gravitational acceleration, h is the depth of the liquid layer, ρ and γ are the liquid's density and surface tension, while k_{mn} is a wavenumber.

Since analytical solutions are limited to regular geometric tank shapes, the case of sloshing in partially filled cylindrical reservoirs has represented over the last 60 years one of the archetypal sloshing systems (Abramson, 1966). In this specific configuration, the wavenumbers

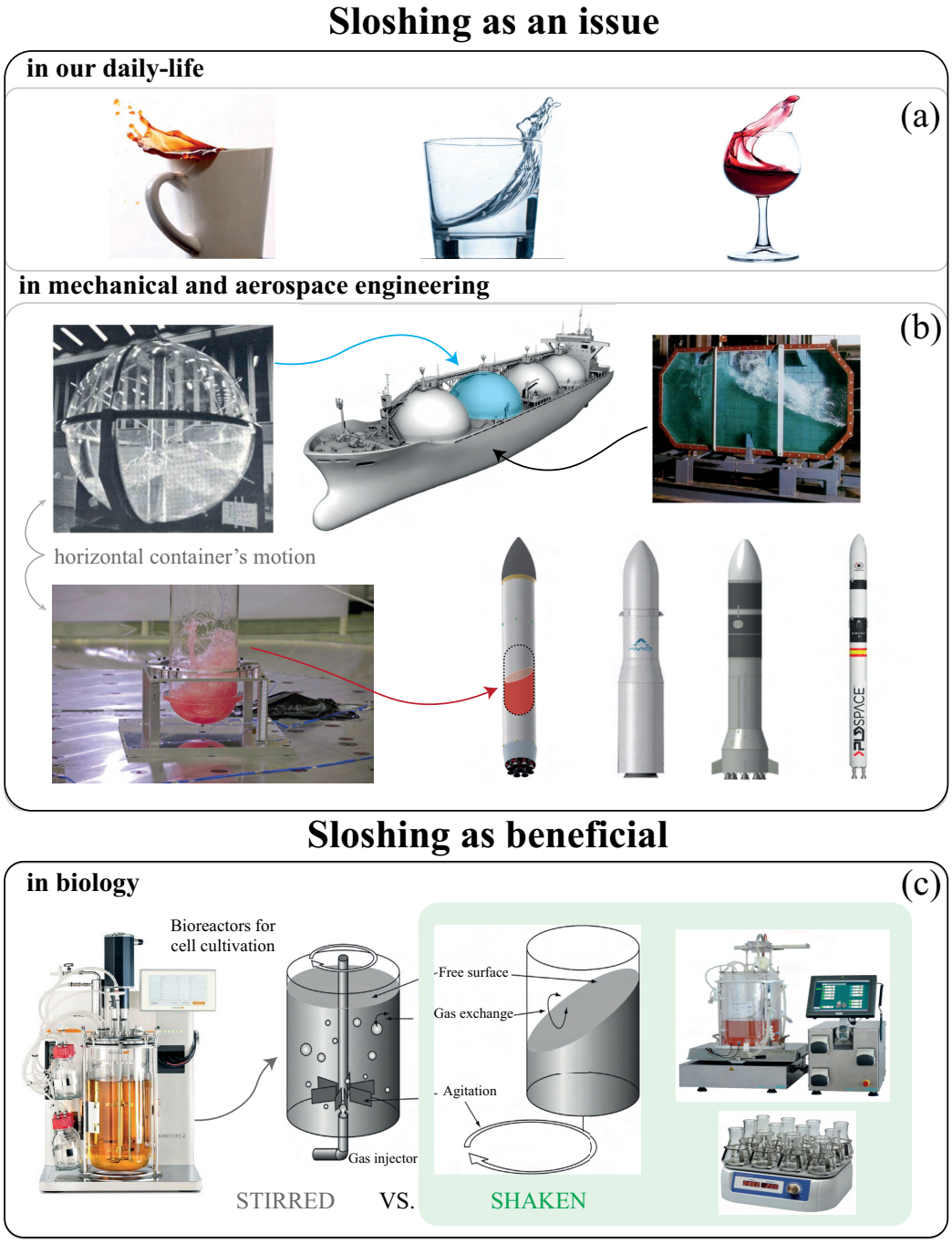

Figure II.1 – (a) Example of daily-life liquid spilling. (b) *Top*, sloshing experiments in large-scale tanks for LNG (liquefied natural gas) carrier (Pastoor et al., 2005). *Bottom*, a sloshing test carried out by ESA (European Space Agency) to test the response of a launcher's liquid propellants to the violence of take-off, so as to better understand the forces involved and enhance future launcher performances. (c) *Left*, stirred tank in operation: gas and chemicals are injected at the bottom, while the agitation is ensured by the propeller, which also breaks the largest bubbles. Gas exchange occurs at the interface of the bubbles. *Right*, orbital-shaken bioreactor: the motion is imposed at the whole vessel, and transmitted to the liquid by the walls, with the gas exchange occurring at the free surface (modified figure from Reclari (2013)).

k_{mn} are given by the nth-roots of the first derivative of the mth-order Bessel function satisfying $J'_m(Rk_{mn})$, with R the container's radius and the indices (m,n) denoting, respectively, the number of nodal circles and nodal diameters of the associated eigenmode. The lowest or first system's natural frequency has typically $(m,n)=(1,1)$ and it is therefore denoted by ω_{11}.

Among all the possible forcing conditions and container trajectories, orbital shaking is particularly interesting, despite its apparent simplicity. Previous experimental studies have carefully described the close-to-resonance dynamics for the two limiting cases, namely circular and purely longitudinal shaking (see figure II.2), casting light on a rich variety of wave regimes, i.e. planar waves, irregular motion or swirling waves, symmetry-breaking, etc., attracting interest to dynamicists over the last decades (Hutton, 1963; Miles, 1984c,d; Ockendon and Ockendon, 1973).

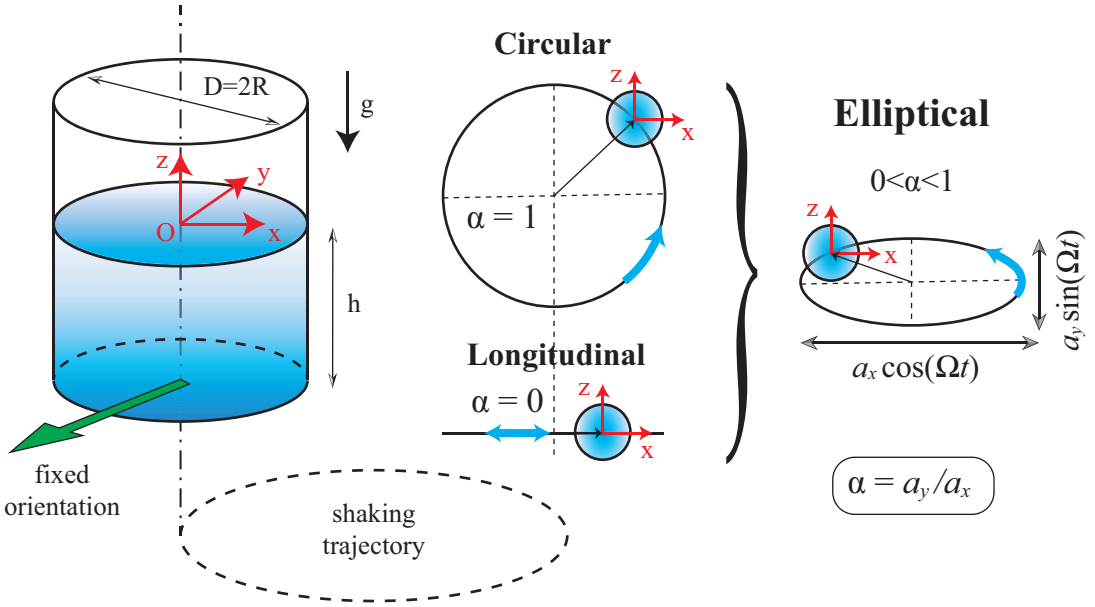

Figure II.2 – Schematic illustration of possible operating parameters of the shaking configurations. Note that the container does not rotate around its own axis, but rather keeps its orientation fixed. The orbit aspect ratio is defined as $\alpha = a_y/a_x$, and it is $\alpha \neq 0$ for a generic *elliptic* orbit. The two limiting cases correspond to $\alpha = 1$, *rotary* shaking, and $\alpha = 0$, *longitudinal* shaking. The external driving is harmonic with angular frequency $\Omega = 2\pi/T$.

For circular orbits, the system responds with a swirling wave always co-directed with the container motion. This well-defined hydrodynamics, often simply modelled by a one-degree-of-freedom Duffing oscillator (Ockendon and Ockendon, 1973), is advantageously exploited in the design of bioreactors for bacterial and cellular cultures (McDaniel and Bailey, 1969; Wurm, 2004), where circular shaking is used as a method to gently mix the liquid content of a container by its displacement at fixed container orientation along a circular trajectory and at a constant angular velocity. Particularly, it constitutes an alternative to stirred tanks (see figure II.1(c)), where the liquid agitation results from a rotating impeller or the rotation of a

	Sub-Harmonic	**Harmonic**	**Super-Harmonic**
ω/Ω	1/2	1	2
ω	$\Omega/2$	Ω	2Ω
Ω/ω	2	1	1/2

Table II.1 – Definition of fundamental sub-harmonic, harmonic and super-harmonic resonances based on the relation between driving frequency, $\Omega = 2\pi/T$, and wave oscillation frequency, ω. The case of sub-harmonic wave responses will be tackled in **Part III** in the context of the parametric Faraday instability.

magnetic rod. In these cultivation protocols, cells are in suspension in the extracellular liquid medium, which serves as buffer for consumables from which they feed and for their secretions. The motion of the liquid prevents sedimentation and homogenizes the concentration of dissolved oxygen and nutrients and of secreted proteins and carbon dioxide. Thanks to the possible gas exchanges at the free surface, oxygen supply from the container bottom can possibly be circumvented, avoiding the formation of bubbles and thereby the damages that their collapse can exert on cells (Handa-Corrigan et al., 1989; Kretzmer and Schügerl, 1991; Papoutsakis, 1991), sparking interest in the development of large-scale, in the hectoliter range, orbital-shaken bioreactors (Jesus et al., 2004; Liu and Hong, 2001; Muller et al., 2007). It is therefore not a surprise if a significant body of research on the gas exchange and mixing in these devices has emerged over the last two decades (Büchs, 2001; Büchs et al., 2000a,b; Maier et al., 2004; Micheletti et al., 2006; Muller et al., 2005; Tan et al., 2011; Tissot et al., 2010, 2011; Zhang et al., 2009).

Since the shear stresses and, therefore, the mixing are proportional to the velocity gradients in the liquid phase, most of the gas exchange phenomena listed above are directly linked to the liquid motion, with the optimal working conditions essentially dictated by the wave pattern (Reclari, 2013). For these reasons, at a more fundamental level, the hydrodynamics of these orbital shaking devices has received recent attention, from both experimental (Bouvard et al., 2017; Moisy et al., 2018; Reclari et al., 2014) and theoretical (Horstmann et al., 2020; Reclari et al., 2014) perspectives, predominantly using linear potential flow models. These models are often complemented with effective viscous damping rates to incorporate the energy dissipation responsible for the phase-shifts between wave and shaker, which was also seen to be sometimes responsible for damping-induced symmetry-breaking linear mechanisms resulting in linear spiral wave patterns (Horstmann et al., 2021, 2020). Previous studies, reviewed for instance in Ibrahim (2005) or Faltinsen and Timokha (2009), make mostly use of classical existing theories for general linear and weakly nonlinear sloshing dynamics in the vicinity of the fundamental harmonic resonance, i.e. when the system is harmonically driven at a frequency close to the lowest natural frequency, ω_{11}.

However, the seminal work of Reclari (2013) cast light on the importance of super-harmonic resonances occurring for an excitation frequency far below ω_{11}, which may possibly manifest with large amplitude responses and wave breaking, hence potentially raising an issue for the robustness of bioreactors if not accounted for. Among these super-harmonics, the double-crest (DC) dynamics (as defined by Reclari (2013)) is particularly relevant, as it displays a

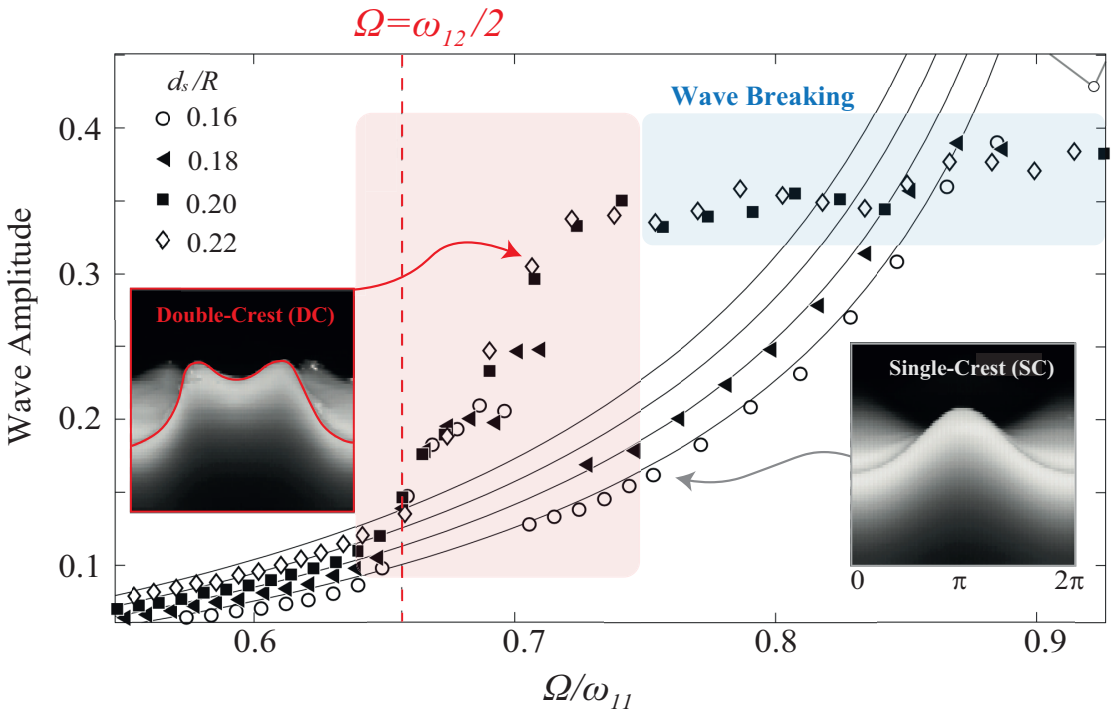

Figure II.3 – Non-dimensional wave amplitude (re-scaled with the container's radius R) between the apparition of super-harmonic double-crested waves (at $\Omega \approx \omega_{21}/2$, vertical red dashed line) and the first system's natural frequency (ω_{11}) (Reclari, 2013). d_s is the orbit of the container's trajectory and represents the dimensional forcing amplitude. The black solid lines correspond to the theoretical predictions given by a linear potential model. The single-crest (SC) and double-crest (DC) wave shapes, visualized along the wall, i.e. $\theta \in [0, 2\pi]$ with θ the azimuthal coordinate, are shown in the two insets (modified figure from Reclari (2013)).

notably large amplitude response, that is strongly favoured by the spatial structure of the external forcing (see figure II.3). In the following we will refer to this resonance as fundamental super-harmonic. To avoid confusion with the contradictory terminology in literature, in table II.1 we define what we mean for fundamental sub-harmonic, harmonic and super-harmonic resonances.

In order to refine the linear potential model and, specifically, to predict the occurrence of the super-harmonic wave dynamics observed experimentally (we remark that by super-harmonic, we mean here a wave of a certain wave frequency ω emerging from an excitation at $\Omega = \omega/2$, with Ω the driving angular frequency), Reclari (2013) and Reclari et al. (2014) proposed an inviscid weakly nonlinear analysis based on a second order straightforward asymptotic expansion procedure, which was shown to be capable of capturing the emergence of the observed resonance. However, their analysis, as typical of straightforward asymptotic expansions, suffers from secular terms (Castaing, 2005; Nayfeh, 2008a) and, therefore, it still fails in describing the correct nonlinear behaviour close to both harmonic and super-harmonic resonances.

With regards to the experiments of Reclari (2013) and Reclari et al. (2014), Timokha and

Raynovskyy (2017) and Raynovskyy and Timokha (2018a,b) have applied the Narimanov-Moiseev multimodal sloshing theory (Dodge et al., 1965; Faltinsen, 1974; Lukovsky, 1990; Moiseev, 1958; Narimanov, 1957; Narimanov et al., 1977). The theory is capable of accurately describing the nonlinear wave dynamics near the fundamental harmonic resonance when no secondary resonances occur (Faltinsen et al., 2016, 2005). Despite the fact that the experiments performed by Reclari (2013) and Reclari et al. (2014) were made for nondimensional fluid depths $H = h/R = 1.04$ and 1, which lie slightly beyond the applicability threshold of the multimodal theory (H_{th} should be $\gtrsim 1.05$ as stated by Raynovskyy and Timokha (2020)) and imposed by the occurrence of secondary resonances, the authors found a quantitative good agreement with the experimental observations associated with the *hardening*-spring type single-crest swirling.

In the spirit of the aforementioned multimodal theory but with regards to square-base basins, the resonant amplification of higher order modes for forcing frequency in the vicinity of the primary resonance (secondary or internal resonances) was investigated by Faltinsen et al. (2005), who formalized a so-called adaptive asymptotic modal approach capable to improve the agreements with earlier experiments. A thorough discussion on this regard is also outlined in chapters 8 and 9 of Faltinsen and Timokha (2009), where the importance of the ratio of tank liquid depth to tank width on the occurrence of the internal resonance phenomenon is carefully discussed. Generally speaking, secondary resonance is a broader concept, and it may occur even far from the primary resonance zone, as in the case of the double-crest swirling observed in Reclari et al. (2014). To our knowledge, the adaptive modal approach was never extended to super-harmonic system responses of orbital-shaken circular cylindrical containers far from the primary resonance.

For these reasons, it appears that a quantitatively accurate model for the prediction of the super-harmonic double-crest (DC) dynamics observed during the thorough experimental campaign carried out by Reclari (2013) and Reclari et al. (2014) has not been provided yet. **Chapter 4** is precisely dedicated to the development of a weakly nonlinear analysis based on the multiple timescale method, which will be seen to successfully capture nonlinear effects for the main additive harmonic resonances as well as the more subtle additive and multiplicative resonance governing the super-harmonic double-crest swirling. Amplitude equations are rigorously derived in an inviscid framework, which once amended with an *ad-hoc* damping term as the only tuning parameter, well match the experimental findings of Reclari (2013) and Reclari et al. (2014). Lastly, the obtained amplitude equations for harmonic single–crest and super-harmonic double–crest waves are found to be compatible with the two well-known one-degree-of-freedom (1dof) systems, the Duffing (already introduced in Chapter 1) and the Helmholtz-Duffing oscillators, respectively.

The study of the double-crest (DC) super-harmonic resonance is extended to longitudinal shaking in **Chapter 5**. The latter forcing condition has been analytically and experimentally studied for decades (Abramson, 1966; Chu, 1968; Hutton, 1963) and it is of interest from the perspective of hydrodynamic instabilities due to the occurrence of hysteretic symmetry-breaking conditions (Miles, 1984a,d). With regards to circular cylindrical containers, particularly rel-

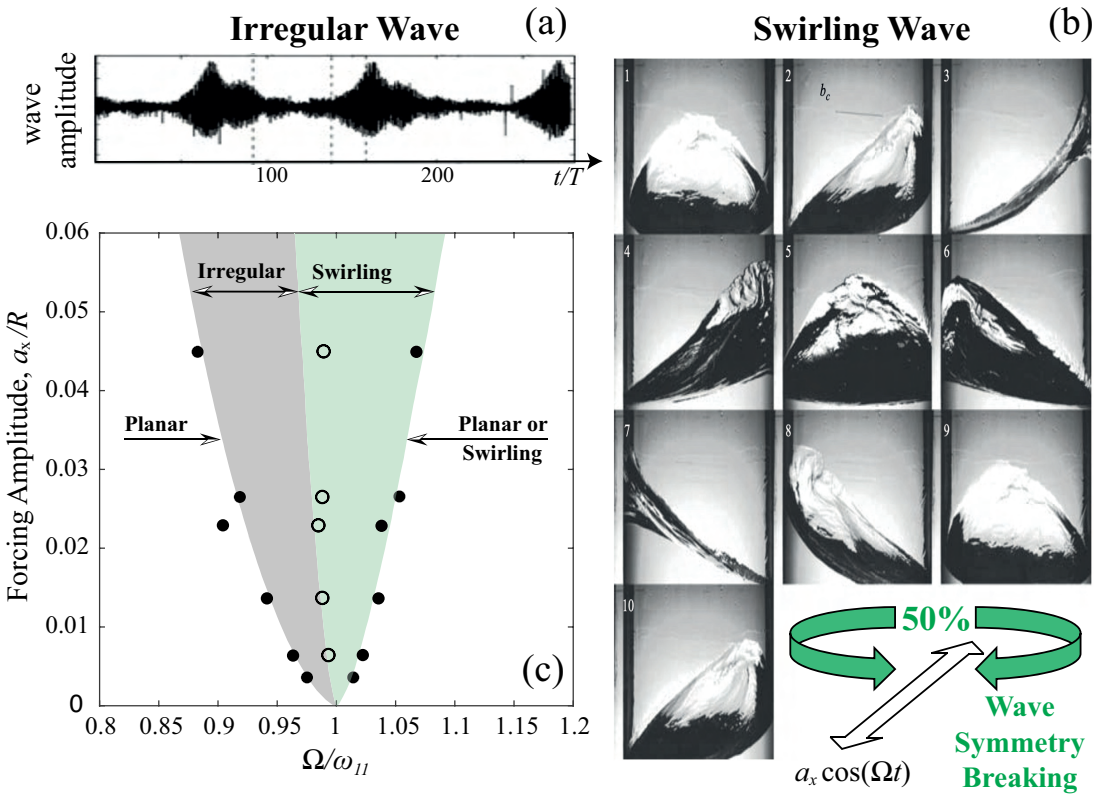

Figure II.4 – (a) Time evolution of the wave amplitude at a probed location in a circular container of radius $R = 78$ mm filled with water to a non-dimensional depth $h/R \approx 1.5$ and undergoing a longitudinal motion of non-dimensional amplitude $a_x/R = 0.0033$ and driving frequency $\Omega/\omega_{11} = 0.98$, with ω_{11} the lowest system's natural frequency. The time series shows a wave envelope modulation occurring on a much larger time scale than the forcing period $T = 2\pi/\Omega$. The absence of a steady wave amplitude regime is a clear sign of irregular motion. (b) Images from Royon-Lebeaud et al. (2007) of a swirling wave in a circular cylinder of radius $R = 150$ mm filled to a depth $h/R \approx 1.2$ and longitudinally forced with $a_x/R = 0.023$ and $\Omega/\omega_{11} \approx 1.02$. Views are in the direction normal to the tank motion. The ten images represent slightly more than one wave period. (c) Theoretical (solid lines, from Faltinsen et al. (2016)) and experimental (circles, from Royon-Lebeaud et al. (2007)) estimates of bounds, in the forcing parameter space, $(\Omega/\omega_{11}, a_x/R)$, between the frequency ranges where planar, irregular and swirling waves occur for close-to-resonance longitudinal forcing conditions, i.e. $\Omega/\omega_{11} \approx 1$.

evant are the experimental studies by Abramson et al. (1966), Royon-Lebeaud et al. (2007) and Hopfinger and Baumbach (2009), who detected the stability bounds between harmonic planar, swirling and irregular waves and whose estimates were later used by Faltinsen et al. (2016) to validate their theoretical analysis (see figure II.4). However, these works were mostly focused on the investigation of system responses in the neighbourhood of harmonic resonances, whereas, with the exception of Reclari (2013); Reclari et al. (2014) in the context of circular sloshing, the literature seems to lack comprehensive experimental and theoretical

studies dealing with the fundamental secondary super-harmonic resonances (discussed in Chapter 4) under longitudinal or, more generally, elliptical container excitation.

In this Chapter, we take a first step in this direction by extending to longitudinal planar forcing the analysis formalized in Chapter 4 for circular container motions. In the spirit of the multiple timescale method, we develop a weakly nonlinear (WNL) model leading to a system of two amplitude equations, whose prediction anticipates that a planar wave symmetry-breaking via stable swirling may also occur under super-harmonic excitation. This finding is confirmed by our experimental observations, which indeed identify three possible super-harmonic regimes, i.e. (i) stable planar DC waves, (ii) irregular motion and (iii) stable swirling DC waves, whose corresponding stability boundaries in the forcing frequency-amplitude plane quantitatively match the present theoretical estimates.

Chapter 5 ends with a brief demonstration of how a straightforward extension of the present analysis to a generic container's elliptic orbit can be readily obtained without any further calculation. This paves the way for the analysis and experimental investigation of the next Chapter, which has been stimulated by the surprising fact that no experimental studies devoted to the more generic case of elliptic container orbits have been reported so far in the sloshing literature. Existing theoretical analyses of this forcing condition brought out interesting features of the resonant liquid response that depend on the orbit's ellipticity. In particular, the inviscid theory of Faltinsen et al. (2016) suggested the counter-intuitive existence, under resonant elliptic forcing, of stable swirling waves that propagate in the direction *opposite* to the forcing direction. Moreover, the theory anticipated that such counter-waves may exist even for quasi-circular orbits and travel with a smaller amplitude than co-directed waves. This, if confirmed, would further enrich the variety of observable dynamical sloshing regimes.

Therefore, **Chapter 6** aims at providing a joint experimental and theoretical characterization of the free liquid surface response for a generic, elliptic periodic container trajectory, so as to bridge the gap between the two diametrically opposed shaking conditions previously discussed. Specifically, with the main focus here on harmonic resonances, we intend to experimentally identify the range of external control parameters, i.e. driving frequency, amplitude and orbit aspect ratio, for which stable counter-directed swirling waves occur. Our findings provide the first strong evidence of the existence of a frequency range where stable swirling can be either co- or counter-directed with respect to the container's direction of motion. Lastly, these results are successfully rationalized and predicted by the inviscid asymptotic model developed in Chapter 5, amended with heuristic damping by analogy with Chapter 4.